Kinetic Monte Carlo investigation of Xe adsorption and desorption on Pt(111) and Pt(997)

B. Lehner, M. Hohage, and P. Zeppenfeld*
Institut für Experimentalphysik, Johannes Kepler Universität Linz, A-4040 Linz, Austria
(Received 14 September 2001; revised manuscript received 6 December 2001; published 4 April 2002)

A discrete event kinetic Monte Carlo (KMC) simulation is applied to model the desorption behavior of Xe on Pt(111) and to study the adsorption and desorption behavior of Xe on the vicinal Pt(997) surface. The simulation results are compared to recent experimental data. For Xe/Pt(111) a phase transition occurs during the desorption, which leads to a change in the desorption behavior from first order for low initial Xe coverage to zero order at higher coverage. The KMC simulation is able to reproduce this transition and hence the experimental desorption spectra by assuming a strongly reduced effective pairwise interaction between neighboring Xe atoms. The vicinal Pt(997) surface presents a nanostructured template substrate, which is well suited to study the influence of step edges and narrow terraces on the adsorption and desorption properties of Xe. Different interaction models were tested by KMC simulations on their ability to reproduce the experimentally observed growth and desorption behavior.

DOI: 10.1103/PhysRevB.65.165407 PACS number(s): 61.43.Bn, 68.43.Fg, 68.43.Mn

I. INTRODUCTION

The adsorption and desorption kinetics of Xe on metal surfaces has been the subject of a large number of experimental[1] and theoretical[2,3] investigations. A main objective has been to understand the binding of Xe to the substrate and the lateral interaction between the adsorbed Xe atoms. In this context, it was noticed that surface defects, such as the unavoidable presence of surface steps, could strongly influence the adsorption and desorption behavior.[4,5] In order to better understand the important role of surface steps, several authors have studied the adsorption and desorption of Xe on regularly stepped (vicinal) surfaces.[5–11] These studies revealed that the step edges present preferential binding sites for the rare gas atoms with a binding energy which can be 20%–60% larger than on the terraces. While such a situation has been observed to occur in many other adsorption systems, like chemisorbed species and metal atoms, other results are quite surprising and have shed new light (and questions) on the nature of the physisorption bond: (i) The rare gas atoms can reach the step edges even at low temperature where the thermal mobility is quite small.[12,13] This ''hyperthermal'' or ''transient'' mobility has been interpreted as being due to the energy gained upon adsorption. This hyperthermal energy cannot be immediately released due to the strong ''phonon mismatch'' between the rare gas atom and the metal substrate.[14–16] (ii) In contrast to the common expectation, Xe atoms may be more strongly bound at the upper rather than the lower step edge. Such a situation has been observed in scanning tunneling microscopy (STM) investigations of Xe/Pt(111),[17,18] whereas for Xe on Cu(110) preferential adsorption at the lower step edge is found.[19] (iii) The stronger binding at the step edge also appears to have a marked influence on the *lateral* interaction between neighboring Xe atoms. In the case of Xe/Pt(111) the attractive interaction between neighboring atoms along the step edge is dramatically reduced and even believed to be repulsive.[5,17] Such a repulsive component could arise from the dipole-dipole interaction—which is expected to increase with the total binding strength—or it could be substrate mediated.[3] The details of the interaction of Xe on metal surfaces are still far from being understood and reliable first-principles studies on the influence of the substrate steps are not yet available.

Perhaps the most intensively studied Xe/metal adsorption system is Xe/Pt(111). Experimental data are available on the trapping and sticking probabilities,[11,20,21] the adsorption-desorption kinetics and interaction strengths,[4,5,11,22–25] the structure and phase diagram,[23–29] the adsorption site,[30,31] the surface mobility,[22,32,33] and the surface phonon dispersion.[34,35] Based on these data, several semiempirical potential models have been proposed,[3,20,36–40] the most refined being the one by Barker *et al.*[39,40] In addition, there exists an *ab initio* cluster calculation for the adsorption of Xe on Pt(111) clusters.[41]

Only recently the adsorption[6–8] and desorption[5] of Xe were studied on the stepped Pt(997) surface which is vicinal to the (111) plane. The experimental data were compared to model calculations and interesting conclusions on the influence of surface steps on both the adsorption and the desorption behavior have been drawn. In particular, the adsorption at intermediate temperatures appears to proceed in a row-by-row fashion. The desorption data provide evidence for strongly modified interaction parameters, such as a repulsive interaction between neighboring Xe atoms adsorbed at the step edges. On the other hand, several issues are still controversial such as the precise nature of the adsorption sites and the adlayer structure and morphology, as well as the relative importance of the contributions of surface kinetics versus thermodynamics to the growth mode and the thermal desorption.

In this context, we have performed kinetic Monte Carlo (KMC) simulations of the adsorption and desorption of Xe on the flat Pt(111) and vicinal Pt(997) surfaces. We have used a novel simulation scheme[42,43] which is capable of dealing with situations close to two-dimensional (2D) equilibrium as well as with processes under the influence of strong kinetic limitations. The aim of this study is to determine the relevant interaction energies and activation barriers and to deduce a consistent model of the underlying atomic processes which is able to describe the experimental data.

II. MONTE CARLO SIMULATION SCHEME

The Monte Carlo simulation scheme is described in Refs. 42 and 43. Only the basic concepts are summarized here: First, thermodynamically consistent energy levels (states) for each adsorbed atom including all accessible adsorption sites are established. The potential energy is determined by the interaction with the surface or underlying layer (allowing for superlattices or defect sites on heterogeneous surfaces) and all neighbors within a given range (not necessarily pairwise or short ranged). In addition, the *transition states* (saddle points) for diffusion and desorption have to be included with their corresponding energies.

On the basis of this energy level diagram, all activation energies are self-consistent and uniquely defined. The probability for a particular event (i.e., the transition rate of an atom of type i from state or position 1 to 2) is defined, as usual, by the Boltzmann factor

$$\nu = \nu_0(1,2) \cdot \exp\left(- \frac{E_i^*(1,2) - E_i(1)}{k_B T} \right), \tag{1}$$

where ν_0 is the preexponential factor and $E_i^*(1,2)$ denotes the energy of the system with atom i in the transition state between initial position 1 [with energy $E_i(1)$] and final position 2. Under these conditions microscopic reversibility (detailed balance) for all diffusion processes (events) is ensured.

Unlike conventional methods we choose the time at which a particular event actually takes place according to the correct time statistics, i.e., using the probability distribution $p(t) = \exp(-\nu t)/\nu$, rather than taking some average time $\langle t \rangle = 1/\nu$. For this purpose, we use an efficient and thoroughly tested random generator[44] providing exponentially distributed random numbers defining the ''event times.'' Using the correct time statistics is essential if time averages are required to determine thermodynamic quantities—such as the chemical potential used, e.g., for the simulation of high-resolution temperature programmed desorption spectra.

All possible events are attributed an event time according to the above scheme. These times are written into a list (time table). The corresponding events are executed in chronological order and the time is propagated accordingly. Since a particular event usually affects the possible transitions at least within a certain neighborhood, the relevant rates have to be recalculated and the corresponding entries in the time table need to be updated. This procedure leads to the correct time statistics of the entire ensemble, provided that the individual events are statistically independent. It also allows ''external'' events (such as adsorption of a particle or the increase of the surface temperature at a given time) to be implemented in a straightforward way.

As a result, the present simulation provides a rigorous description of the time evolution of the simulated system. Thus *by construction* a ''dynamical hierarchy'' of transition probabilities and the correct ''physical time scale'' ensuring a detailed balance is provided. The simulation box needs to be sufficiently large that single-site and intersite correlations are lost and the events are statistically independent.[45]

III. DESORPTION OF Xe FROM Pt(111)

Xenon physisorbs on the Pt(111) surface with attractive interactions between neighboring Xe atoms. For the unconstrained monolayer, i.e., in the 2D-gas–solid coexistence regime, an isosteric heat of adsorption of $Q_1 = 298 \pm 22$ meV (average from Refs. 5, 11, and 22–24) has been reported. At low coverage, an average value of $Q_0 = 260 \pm 15$ meV is obtained.[4,5,11,22–24] The difference of about 30–40 meV is related to the 2D condensation enthalpy Q_{2D} of the 2D solid. This 2D heat of condensation has also been measured directly using He atom scattering, yielding slightly larger values of $Q_{2D} = 43$ meV (Ref. 25) and $Q_{2D} = 48$ meV (Ref. 23). The measured values (enthalpies) Q_0 and Q_{2D} can be related, respectively, to the binding energy E_{ter} of a single Xe atom to the Pt(111) substrate and to an *effective* nearest-neighbor Xe-Xe binding energy E_{lat}. Within an error of $k_B T$ (which is of the order of 5–10 meV in the present case), $E_{ter} \simeq Q_0$ and $E_{lat} \simeq Q_{2D}/3$ for a hexagonal lattice with nearest-neighbor coordination of 6. Therefore, we expect that the adsorption of Xe on Pt(111) should be correctly modeled using values of $E_{ter} = 250$–270 meV and $E_{lat} = 10$–16 meV. A third parameter, the diffusion barrier E_{dif}, is required to describe the surface mobility and hence the surface kinetics. In the present simulation scheme, E_{dif} for an isolated Xe adatom is obtained from the energy difference of the initial binding site and the transition state (saddle point) E_{sad}, i.e., on the flat Pt(111) terrace $E_{dif} = E_{sad} - E_{ter}$. Note that the activation energy for diffusion increases by nE_{lat} if n nearest-neighbor bonds have to be broken to move into the transition state, e.g., if the Xe atom is detached from an existing Xe cluster or island. From the temperature dependence of the Xe island density and island coarsening,[32] the activation barrier for single-adatom diffusion was estimated to be of the order of 31 meV, whereas the activation energy involving island detachment was found to be 64 meV. Assuming detachment from kink sites involving the breaking of three nearest-neighbor Xe-Xe bonds, this value is consistent with an effective nearest-neighbor attraction of $E_{lat} = 11$ meV. Finally, the preexponential factors ν_{jump} and ν_{des} for jump diffusion and desorption, respectively, have to be defined in order to evaluate the hopping and desorption rates using Eq. (1). Typical values for these preexponential factors (attempt frequencies) range between 10^{12} s^{-1} and 10^{13} s^{-1}, matching the corresponding lateral and perpendicular vibration frequencies. Under the conditions relevant for the desorption experiments simulated below (surface temperature above 60 K and coverages below one monolayer) Xe will form a commensurate $(\sqrt{3} \times \sqrt{3})R30°$ superstructure on the defect-free Pt(111) surface.[46] This commensurate phase is easily modeled in the simulation assuming a perfect 2D substrate lattice.

The experimental temperature programmed desorption (TPD) spectra of submonolayer Xe on Pt(111), reported by Widdra *et al.*,[5] reveal an unusual behavior within the first monolayer (see Fig. 1): Whereas for higher initial coverages zero-order desorption is observed (characterized by a common leading edge), at low initial coverage ($\Theta \lesssim 10\%$ of a monolayer), the desorption seems to follow a first-order be-

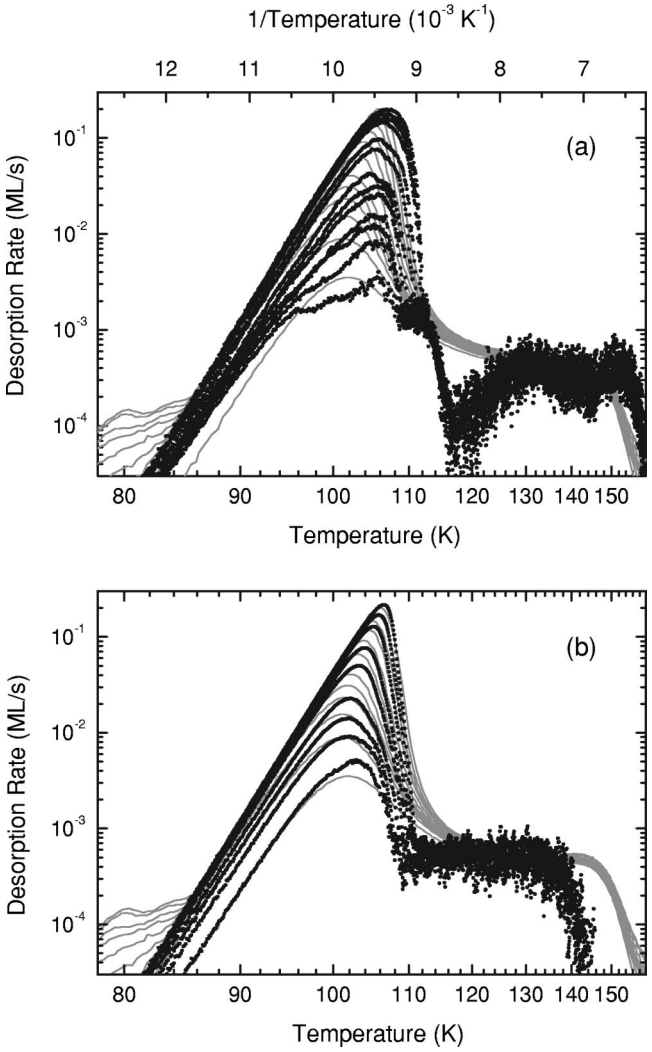

FIG. 1. TPD spectra of Xe on Pt(111) for different initial coverages ranging between 0.03 and 1 monolayer. Thin solid lines: experimental data (Ref. 5), Menzel-Schlichting plot, courtesy of W. Widdra. Black dots: simulated data, parameters according to Table I, assuming (a) severe kinetic limitations and (b) a reduced lateral interaction (see text for details). The small shoulder to the very right is due to desorption from residual step edges. Heating rate: 2 K/s.

TABLE I. Simulation parameters for the desorption of Xe/Pt(111). (a) and (b) refer to simulations assuming large kinetic limitations and reduced lateral interactions, respectively. E_{ter}: binding energy of a single Xe atom on the Pt(111) terrace. E_{lat}: lateral interaction energy between two neighboring Xe adatoms on the terrace. Note that in both cases (a) and (b) the total energy in the 2D solid phase is the same: $E_{ter}+3E_{lat}=277.3$ meV. The saddle point (intermediate state) for diffusion is located at an energy E_{sad} below the vacuum level. ν_{jump} and ν_{des} are the attempt frequencies for diffusion and desorption, respectively. As discussed in Ref. 42 Xe atoms in the second layer have also to be taken into account. The corresponding binding energies are derived from the kink energy in the bilayer E_{BL} assuming nearest-neighbor pairwise interactions. The bottom part lists the additional parameters describing the interaction at step edges (a step density of 1/128 adsorbate rows was assumed in Fig. 1). The actual values were suggested in Ref. 5. E_{top},E_{bot}: binding energies of a Xe atom on the top and at the bottom of a step edge, respectively. E_{tt},E_{bb}: lateral interaction between neighboring Xe atoms within the top and bottom rows at the step edge, respectively. E_{t*},E_{b*}: lateral interaction between Xe atoms in the top (bottom) row and a neighboring atom on the upper (lower) terrace. E_{tb}: interaction between nearest Xe atoms in the top and bottom rows.

Parameter	(a)	(b)
E_{ter}	243.7 meV	256.3 meV
E_{lat}	11.2 meV	7.0 meV
E_{sad}	0 meV	95 meV
E_{BL}	170 meV	
ν_{jump}	6×10^{12} s^{-1}	
ν_{des}	1.8×10^{13} s^{-1}	
	Step edges	
E_{top}	402.2 meV	
E_{bot}	291.2 meV	
E_{tt}	-15.9 meV (repulsive)	
E_{bb}	11.2 meV	
E_{t*}	-4.3 meV (repulsive)	
E_{b*}	4.3 meV	
E_{tb}	0 meV	

havior, where the desorption maxima are located at the same temperature and the leading edge is shifted to higher temperature. The initial first-order behavior can be explained by the existence of a single-phase regime (2D gas). Above a certain critical coverage a 2D solid phase coexists with the 2D gas phase, leading to zero-order desorption. Alternatively, the initial first-order desorption might also be caused by severe kinetic limitations of the Xe diffusion within the first monolayer.[5,42] In the first case, the change in desorption order would be an equilibrium phenomenon related to the 2D-gas–solid transition and, hence, it would be governed by the effective lateral interaction between neighboring Xe atoms. In the second case, the phenomenon would be a kinetic one, originating from a large barrier for diffusion of the Xe atoms across the Pt(111) surface.

Up to now, a rate equation based interpretation of the TPD spectra[5] has assigned the initial first-order desorption behavior to a kinetic limitation of the adsorbate on the uncovered surface. In fact, a kinetic limitation of this type is able to reproduce the desired effect.[5,42] In order to lead to a first order desorption signature, the strength of such a kinetic limitation has to be high enough, to inhibit 2D gas formation on the uncovered Pt substrate at the desorption temperature,[43] while the 2D gas formation and adsorbate motion on top of existing Xe islands remains active. Indeed, a reasonable fit to the TPD spectra can be achieved by introducing kinetic limitations. The corresponding simulation results, using the parameter values listed in Table I(a), are plotted in Fig. 1(a). Note, however, that the activation energy for the diffusion of Xe on the Pt(111) substrate needs to be almost as high as the particle binding energy on the substrate ($E_{sad}=0$) (Refs. 5 and 43)—but at least larger than 200 meV.[47] Such a huge diffusion barrier would also inhibit Xe island formation on Pt(111) at lower temperatures in strong

disagreement with the experimental observation of large island formation even below 40 K. Indeed, according to He diffraction and STM studies on Xe island growth[25,32] the diffusion barrier should rather be of the order of 30 meV.

Another possibility to reproduce the shift from first- to zero-order desorption with increasing initial coverage is to determine a lateral attraction which yields the right critical coverage and temperature for the 2D-gas–solid transition. From measurements of the critical temperature $T_c \approx 120$ K and the 2D heat of condensation, one would infer a pairwise effective lateral interaction of about 11–15 meV.[23,26] Using, instead, a lateral interaction of 7 meV between nearest Xe atoms as in Ref. 5 gives an excellent match of the simulated spectra to the experimental data [see Fig. 1(b) for the parameter values listed in Table I(b)]. Note that in this case the diffusion is high enough to maintain 2D equilibrium throughout the entire desorption process.[43]

Besides the binding energy on the terrace we have also included the parameters describing the interaction of the Xe atoms at residual step edges which were incorporated explicitly in the simulation lattice.[43] The interaction parameters in the vicinity of the step edges (listed in Table I) were taken to be the same as on the vicinal Pt(997) surface (model No. 4 described below). The stronger binding to the step edges and the characteristic modification of the Xe-Xe lateral interaction at the step edges are responsible for the broad desorption feature located between 120 and 140 K. The intensity relative to the main desorption peak is well reproduced for a residual step density of about 0.5% (one edge every 128 close-packed Xe rows).

Combinations of kinetic limitations and reduced lateral interactions turn out to be not very promising, since sizable effects due to kinetic limitations do only occur for quite high and, hence, unrealistic diffusion barriers.[47] On the basis of our simulation results we may, therefore, conclude that kinetic limitations are unlikely to be responsible for the observed transition from first- to zero-order desorption but that it is rather due to the transition from the 2D gas to solid phase. Nevertheless, we have to worry about the small lateral interaction energy of only 7 meV which is required to fit the experimental spectra. In fact, the difficulty is to reproduce the surprisingly high 2D-gas densities in the KMC simulation (several percent of a monolayer at 100 K) up to which first-order desorption still occurs. This difficulty may be due to the oversimplified Xe-Xe interaction model (with only a nearest-neighbor term E_{lat}) used in the present simulation:

(i) The simple relation between the critical temperature T_c and the lateral interaction E_{lat} only holds for certain lattice gas interaction models.[3,48] Other (long-range) contributions, like three-body and substrate-mediated interactions, may lead to much larger fluctuations between the 2D-gas phase and 2D-solid phase and to a significant increase of the equilibrium 2D-gas phase density.[49] KMC simulations are currently performed to study the possible influence of such long-range contributions to the lateral interactions on the desorption behavior.[50]

(ii) Lateral interactions as determined from the 2D heat of condensation are measured at lower temperatures (typically 60–90 K) than during desorption (≈ 100 K). As a result, the respective island sizes are different. More precisely, the adsorption experiments measure the coalescence energy of large commensurate 2D islands, whereas close to desorption the remaining 2D islands will be rather small. Due to the Xe-Pt lattice mismatch, such small 2D Xe clusters may effectively relax the lateral strain (especially along the island borders), resulting in a lower energy for the attachment of an additional Xe atom from the 2D-gas phase. This reduced attachment energy, however, determines the effective lateral interaction and, hence, the 2D-gas density.

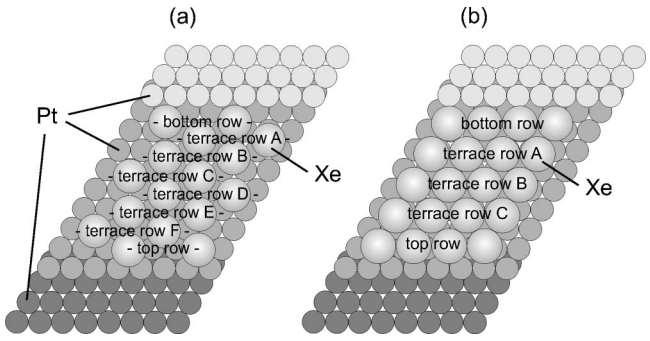

FIG. 2. Schematic of the Xe adlayer structure on the vicinal Pt(997) surface. (a) $(\sqrt{3}\times\sqrt{3})R30°$ structure with eight rows per terrace, in analogy to the Xe adlayer structure on the flat Pt(111) surface. (b) $R0°$ aligned incommensurate phase with five rows per terrace, as inferred from LEED and He diffraction data (Refs. 5, 7, and 53).

Only recently, KMC simulations have demonstrated the important effect of long-range interactions on the island nucleation and growth in the case of strained Ag adlayers on Pt(111).[51] Similar efforts should be devoted to a more accurate modeling of the lateral interactions in physisorption systems. Work in this direction is currently in progress.

IV. Xe ADSORPTION ON Pt(997)

The Pt(997) vicinal surface consists of a regular array of Pt(111) terraces of 20.4 Å width, which are separated by $(11\bar{1})$-oriented monatomic steps (see Fig. 2). Xe on Pt(997) thus provides a model system for studying the influence of step defects and the reduced terrace width on the adsorption and desorption behavior.

The adlayer equilibrium structure is closely related to the details of the adsorbate-substrate and adsorbate-adsorbate interaction potentials. Yet the interaction of Xe atoms near step edges is not fully understood at the moment. For Pt(111) it is known that Xe atoms prefer to adsorb on top of an existing step edge.[17,18] Recent He scattering experiments, however, seem to indicate that on Pt(997) the preferred position for a Xe atom is at the bottom of the step edge.[6,7] Moreover, the monolayer structure of Xe on Pt(997) is still controversial.[7] At first, one might expect a $(\sqrt{3}\times\sqrt{3})R30°$ commensurate or incommensurate phase, both rotated by 30° with respect to the substrate, as on the flat Pt(111) surface.[26,52] In this structure eight Xe rows parallel to the step edges would fit on each Pt terrace [Fig. 2(a)]. However, a different structure was suggested from low-energy electron diffraction (LEED) and

He diffraction.[5,7,53] According to these experiments, Xe forms a quasihexagonal $R0°$-*aligned* incommensurate phase, which is compressed as compared to the $(\sqrt{3}\times\sqrt{3})R30°$ structure observed on large Pt(111) terraces. Along the close-packed Xe rows running *parallel* to the Pt step edges the Xe atoms are separated by 4.1 Å and the distance between neighboring rows is 3.87 Å. In this structure five close-packed Xe rows can be accommodated on each terrace of the Pt(997) surface [Fig. 2(b)].

At low coverage, when the steps are decorated by a single Xe row, the structure was found to be commensurate with a Xe spacing of $2a_{Pt}=5.54$ Å along the step.[5,6,12] Still, the authors disagree on the adsorption site being at the top or at the bottom of the step edge. He scattering experiments under grazing incidence indicate a row-by-row growth for the first two adsorbed Xe rows: a clear intensity peak characteristic for the growth of a distinct second row is observed below 70 K (see, e.g., Fig. 1 in Ref. 6). In the following, KMC simulations of the adsorption of Xe on Pt(997) are presented using four different interaction models. These models will be judged especially by their ability to reproduce the sequential growth of the first two Xe rows.

A. Model No. 1

In analogy to the Xe adlayer structure observed on Pt(111), a $(\sqrt{3}\times\sqrt{3})R30°$ structure has been used to theoretically model the row-by-row growth of Xe on the Pt(997) surface.[7] This structure is illustrated in Fig. 2(a). Note that the spacing between Xe atoms along each row, i.e., the Xe-Xe distance along the step edge, is $3a_{Pt}$ and eight Xe rows can be placed on each Pt terrace for monolayer completion. One row right at the step edge is considered to be energetically preferred. For this model it is irrelevant whether the preferred sites are located on top or at the bottom of the step edge; the same growth scenario is obtained—just the growth direction away from the step edge is reversed. In the present case, we have chosen the top of the step edge to be energetically preferred by 134 meV with respect to the terrace sites. All simulation parameters for this model are listed in Table II.

The partial Xe coverages in each row, obtained from KMC simulations for 60 K and 80 K, are shown in Fig. 3. Notice that for a complete Xe monolayer of the $(\sqrt{3}\times\sqrt{3})R30°$ phase the total (2D) coverage as well as the (1D) coverage within each complete Xe row is 0.33. Figure 4 sketches a sector of the simulated adlayer structure for different total coverages. As can be seen from Figs. 3 and 4, the Xe atoms preferentially build a ''distance-2'' structure within the energetically preferred top row. This allows more atoms to benefit from the additional step energy, then for a distance of $3a_{Pt}$ in the $(\sqrt{3}\times\sqrt{3})R30°$ structure. The neighboring row (terrace row F) is populated only at a few sites, near defects in the distance-2 order of the top row. Before the second row is completed the third and subsequent rows start to be filled, forming patches of the $(\sqrt{3}\times\sqrt{3})R30°$ structure without changing the configuration within the top row.

As a result, no row-by-row growth does occur at any temperature. Instead, a ''Stranski-Krastanov'' growth is ob-

TABLE II. Parameters for the KMC simulations of the adsorption and growth of Xe on Pt(997) for the four different models described in the text. All energies are in meV, the jump frequency ν_{jump} in s^{-1}. Different saddle points for diffusion within the top row $E_{sad\ top}$ and all other jumps $E_{sad\ terrace}$ have been used.

Model structure	No. 1 Fig. 2(a)	No. 2 Fig. 2(a)	No. 3 Fig. 2(b)	No. 4 Fig. 2(b)
$E_{bottom\ row}$	264	352	264	287
$E_{terrace\ row\ A}$	264	260	264	264
$E_{terrace\ row\ B}$	264	255	264	264
$E_{terrace\ row\ C}$	264	255	264	264
$E_{terrace\ row\ D}$	264	255	-	-
$E_{terrace\ row\ E}$	264	255	-	-
$E_{terrace\ row\ F}$	264	250	-	-
$E_{top\ row}$	398	226	398	398
E_{lat}	11.2	11	11.2	[a]
$E_{sad\ terrace}$	234	220	234	234
$E_{sad\ top}$	234	220	368	368
ν_{jump}	6×10^{12}	6×10^{12}	6×10^{12}	6×10^{12}

[a]The lateral interaction within model No. 4 depends on the position of the two adsorbate atoms. $E_{lat}=11.2$ meV is only valid if both atoms are located on terrace rows. In the other cases the same interaction parameters E_{tt}, E_{bb}, E_{t*}, E_{b*}, and E_{tb} as in Table I have been used.

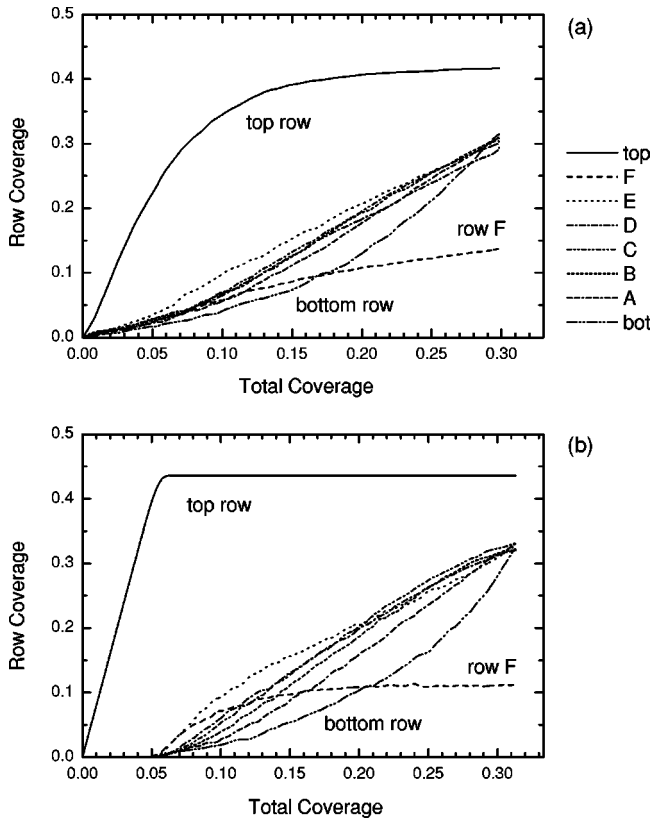

FIG. 3. 1D coverages of different rows vs total (2D) coverage from KMC adsorption simulations at (a) 60 K and (b) 80 K, using interaction model No. 1 (for parameters see Table II).

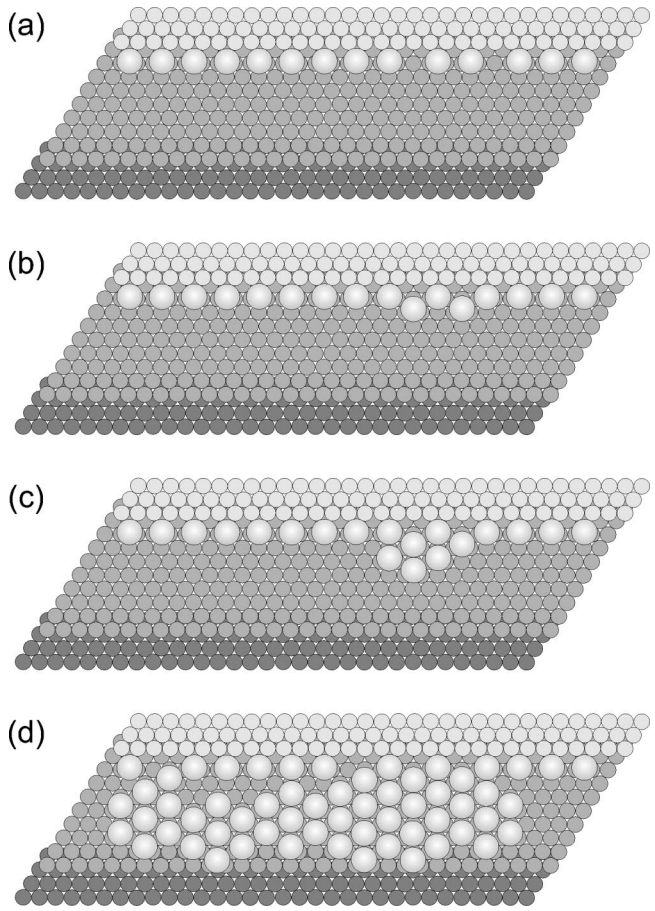

FIG. 4. Schematic of the growth of Xe on Pt(997), using interaction model No. 1 and the corresponding $(\sqrt{3}\times\sqrt{3})R30°$ structure. The sequence (a)–(d) sketches the typical scenario observed in the KMC simulation.

served, in which only a *single* row is more or less completed before $(\sqrt{3}\times\sqrt{3})R30°$ islands are formed on the terraces. This is due to the fact that the first row takes a denser structure with an interatomic distance of $2a_{Pt}$ in order to take advantage of the increased Xe-Pt attraction at the step edge. On the other hand, the lateral interaction favors the $(\sqrt{3}\times\sqrt{3})R30°$ phase, which is therefore established on the terraces once the step edge is decorated. Due to this large lattice mismatch, the $(\sqrt{3}\times\sqrt{3})R30°$ phase cannot completely wet the first row.

B. Model No. 2

This model, suggested by Pouthier *et al.* in Ref. 7, assigns individual adsorbate-substrate interaction energies for the eight different Xe rows within the $(\sqrt{3}\times\sqrt{3})R30°$ structure. The potential shows a steady increase from the bottom row (considered as the energetically favored row) to the row on top of the step edge, in which the Xe are most weakly bound. The corresponding simulation parameters are given in Table II.

Looking at the simulation results for 60 K and 80 K, shown in Fig. 5, the expected preferential growth of the bottom row is clearly evident, especially at higher temperature.

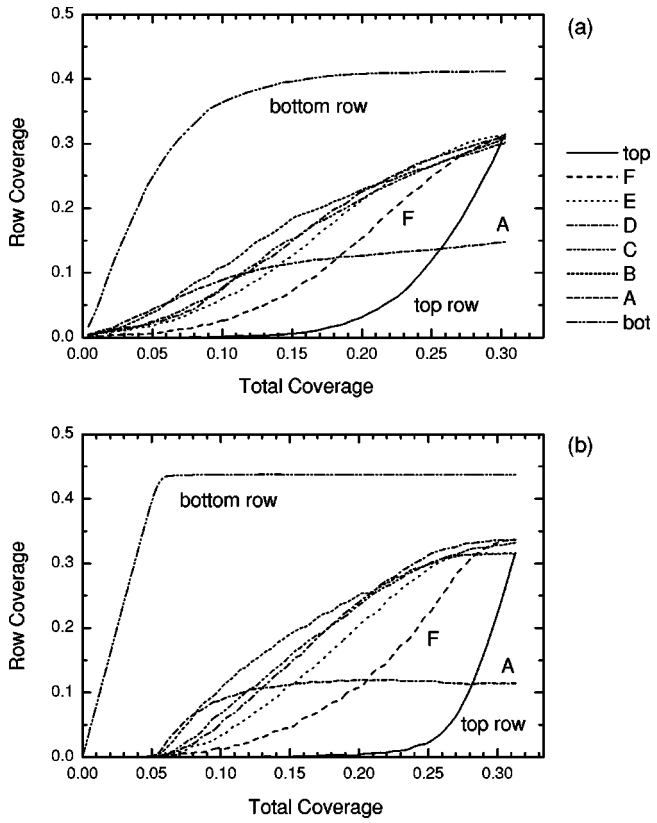

FIG. 5. 1D coverages of different rows vs total (2D) coverage from KMC adsorption simulations at (a) 60 K and (b) 80 K, using interaction model No. 2 (for parameters see Table II).

The neighboring terrace row *A* grows next, but well before its completion, the third terrace row *B*, and all subsequent terrace rows become more populated than terrace row *A*. The top row is populated last, due to the low Xe binding energy to the substrate and the additional lack of two lateral Xe neighbors. As with model No. 1 above, this is again the signature of a ''frustration,'' intrinsic to all models based on the $(\sqrt{3}\times\sqrt{3})R30°$ structure, namely, the mismatch between the denser Xe row at the step edge ($\Theta=0.5$) and the $(\sqrt{3}\times\sqrt{3})R30°$ phase with line density ($\Theta=0.33$). This only allows a few sites to be occupied within terrace row *A* before island formation sets in. A row-by-row growth of the first two rows is never achieved with this model, even though the terrace row *A* is slightly favored by 5 meV with respect to the next terrace row *B*.

C. Model No. 3

According to the diffraction experiments,[5,7,53] xenon forms an incommensurate $R0°$ structure with five close-packed Xe rows fitting on a single terrace of the Pt(997) surface [see Fig. 2(b)]. KMC simulations using the adsorbate pseudolattice, defined by the positions of the Xe atoms in this ideal quasihexagonal structure, have been performed. The interactions and the binding preference to the step edge are the same as in model No. 1 but the structure of the growing adlayer is quite different. The simulation parameters for this model are given in Table II.

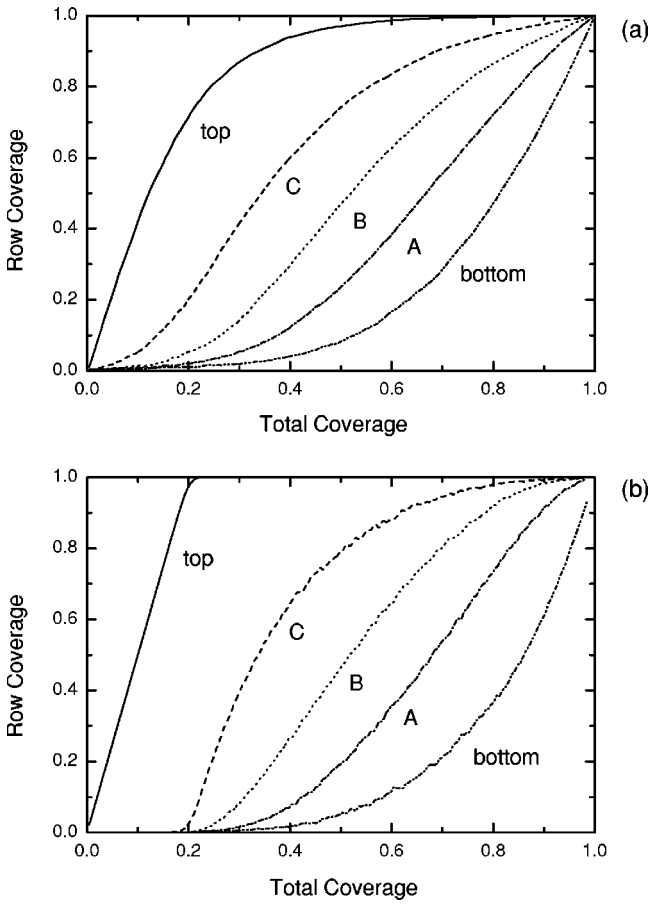

FIG. 6. 1D coverages of different rows vs total (2D) coverage from KMC adsorption simulations at (a) 60 K and (b) 80 K, using interaction model No. 3 (for parameters see Table II).

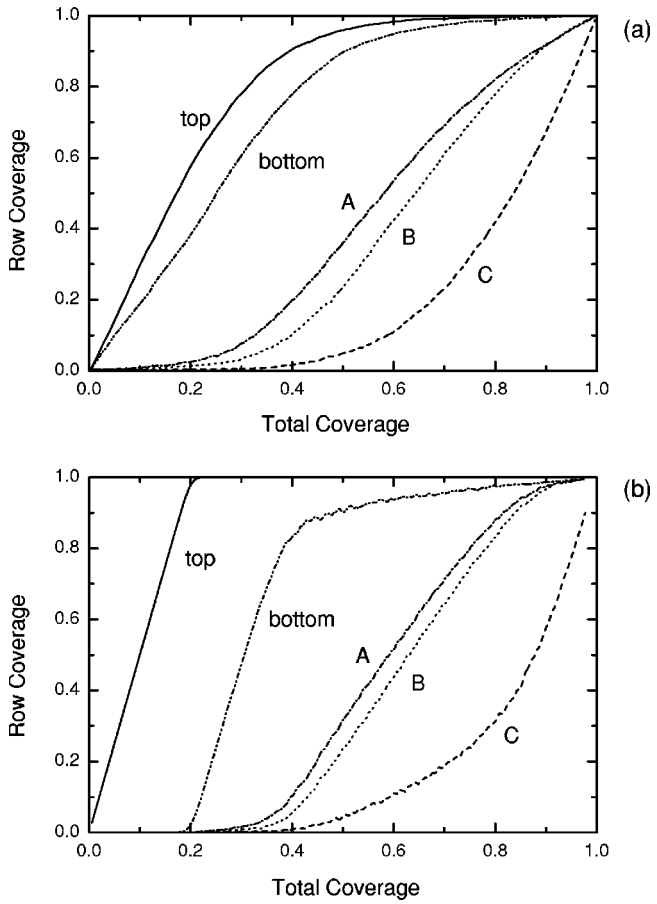

FIG. 7. 1D coverages of different rows vs total (2D) coverage from KMC adsorption simulations at (a) 60 K and (b) 80 K, using interaction model No. 4 (for parameters see Table II).

The growth behavior is best characterized by the partial coverages within each row, as a function of the total coverage. Figure 6 shows the results of the KMC simulations for adsorption temperatures of 60 K and 80 K. For both temperatures, the energetically preferred top row is occupied first. At 80 K the first row is filled up completely, before the other rows even start to grow. At 60 K not all atoms are able to reach this row, and the other rows start to be occupied earlier. With increasing exposure one can observe the completion of the three terrace rows and, eventually, the growth of the bottom row. Since the Xe atoms in the bottom row have a maximum of only four lateral neighbors instead of six within the terrace rows, the bottom row is energetically most unfavorable.

In contrast to model Nos. 1 and 2, at least a partial wetting of the first row by a second row can be obtained as shown by the initial steep increase of the partial coverage of terrace row *C* after completion of the top row [see Fig. 6(b)]. Indeed, there is no lattice mismatch between these two rows as in the models based on the $(\sqrt{3}\times\sqrt{3})R30°$ structure. Nevertheless, the driving force for the attachment of Xe atoms next to the completed first row, i.e., the lateral interaction $2E_{lat}=22.4$ meV, is rather small. In fact, a straightforward way to enforce the subsequent growth of a neighboring row is to increase the binding strength to the substrate within terrace row *C* or, alternatively, within the bottom row.

D. Model No. 4

The last interaction model to be presented was suggested by Widdra *et al.*[5] It is defined for the same aligned adlayer structure as model No. 3 but the interaction energies are such that adsorption sites within the top row and (to a lesser extent) also at the bottom of the step are energetically favored with respect to the terrace sites (Table II). In addition, a repulsion between neighboring Xe atoms adsorbed within the top row and for atoms approaching it from the upper terrace is introduced (see ''Step edges'' in Table I). The hierarchy of the binding strengths and the lateral repulsion were motivated by the STM observations on the growth of Xe at the residual step edges on the Pt(111) surface.[17,18] Again KMC growth simulations have been performed at different temperatures. The results for 60 K and 80 K are shown in Fig. 7.

Due to the stronger binding, the top and bottom rows are the first ones to grow. At 80 K [Fig. 7(b)] a distinct row-by-row growth of the first two rows is observed. At the lower temperature of 60 K both rows grow nearly at the same time and are almost completed before the remaining terrace rows are occupied. Due to the lateral repulsion of the Xe atoms

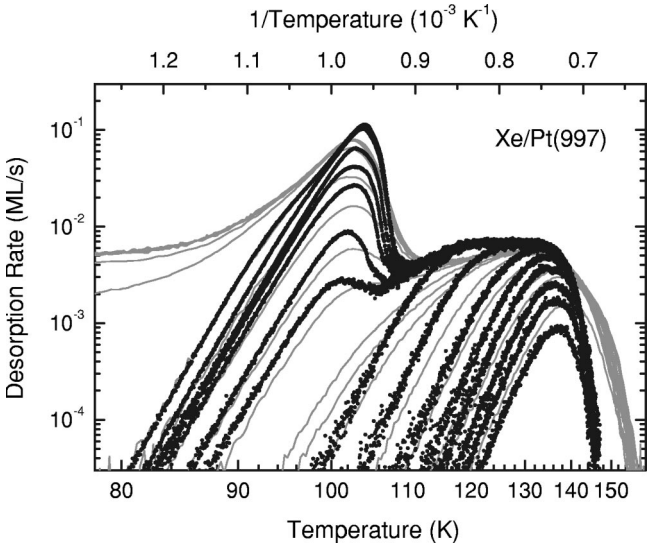

FIG. 8. TPD spectra of Xe on Pt(997). Thin solid lines: experimental data (Ref. 5), Menzel-Schlichting plot, courtesy of W. Widdra. Black dots: simulated data, parameters according to model No. 4 listed in Table II. The monolayer desorption peak splits into a peak containing about 80% of the total monolayer coverage, and a broad shoulder with an integrated intensity of about 20% of a monolayer. Heating rate: 1 K/s.

located within the top row to neighboring atoms on the upper terrace, row *C* is energetically unfavored and filled up last. The strong preferential binding within the top and bottom row should give rise to a strong peak in the reflected He intensity after completion of the first and second rows. This is, indeed, observed experimentally (see Fig. 3 in Ref. 6). The details of the growth depend on the size of the repulsion within the top row (-15.9 meV) and the choice of the saddle points for diffusion will be discussed in Sec. V. Finally, the chosen quasilattice does not allow for the energetically favored commensurate structure along the step edges, with a lattice spacing of $2a_{Pt}$. Since the repulsion in this structure is strongly reduced, the growth of an uncompressed top row should be energetically favored. Hence, the sequential growth of the top and bottom rows is expected to be even more distinct.

V. DESORPTION OF Xe FROM Pt(997)

While the results of the adsorption simulations based on model No. 4 are in good agreement with the experimental results of Refs. 6 and 7, the step edge interaction parameters given in Table I cannot be uniquely determined from the comparison of the adsorption data alone. In fact, these parameters have been proposed by Widdra *et al.*[5] on the basis of a rate equation analysis of *desorption* spectra of Xe on the Pt(997) surface: it turns out that the shape of the desorption curves is quite sensitive on the interaction of Xe at the steps.

The experimental TPD curves from Ref. 5 are shown in Fig. 8 (thin solid lines). The submonolayer desorption spectra consist of a main peak with a maximum at about 103 K and a broad shoulder at higher temperature (between 115 K and 145 K). The integrated peak area (i.e., the partial coverage) of the shoulder is about 20% of a monolayer, while the main peak contains the remaining 80%. As a consequence, one can attribute the shoulder to the desorption from a single Xe row with an additional binding energy, on top or at the bottom of the step edge, whereas the main peak thus corresponds to the desorption from four terrace rows. This provides additional support for the five-row structure of the aligned phase (model Nos. 3 and 4) in contrast to the eight-row model associated with a $(\sqrt{3}\times\sqrt{3})R30°$ structure. For low initial coverages only the high-temperature desorption feature is observed. Its peak position shifts to lower temperatures with increasing initial coverage. This indicates a sizable *repulsive* lateral interaction between the Xe atoms adsorbed at the step edge.[5,17] Finally, the main desorption peak shows a first-order behavior even at high initial coverage, in contrast to the zero-order desorption observed on the extended terraces on Pt(111) (see Fig. 1). This difference is related to the finite size of the (111) terraces on the Pt(997) surface and the strong influence of the step edge on the size and shape of the 2D Xe islands.

KMC simulations of the Xe desorption from the Pt(997) surface were performed on the basis of model No. 4, already used in the adsorption studies. The same conditions (five Xe rows per terrace, adsorbate pseudolattice, interaction parameters as listed in Tables I and II) were used. The simulated TPD spectra are shown in Fig. 8 as the small dots. A quantitative agreement between experiment and simulation is obtained. In particular, the main characteristic features are well reproduced by the simulation: (i) the nearly first-order desorption of Xe from the Pt terraces in the main peak, (ii) the relative peak areas and intensities corresponding to the desorption from the terraces and step edges, respectively, and (iii) the broad characteristic shape of the shoulder, originating from the lateral repulsion within the top row.

VI. DISCUSSION

A. Reliability and relevance of the simulation parameters

A KMC simulation requires a set of parameters representing the most important aspects of the potential energy surface experienced by the adatoms: binding energies depending on the adsorption site and the configuration of neighbors, transition-state energies for motion between such sites and the corresponding attempt frequencies [see Eq. (1)].

In principle, there are three different sources from which appropriate parameter values may be obtained: (i) Parameters can be determined directly from experiments, e.g., from desorption spectra or adsorption isotherms. However, not all required quantities are easily accessible from experimental data. (ii) Parameters can be taken from *ab initio* calculations. Unfortunately, such calculations for adatoms adsorbed on vicinal surfaces require large unit cells and, therefore, immense computational effort. (iii) Finally, parameters can be extracted by fitting simulation results to experimental data. As most phenomena can be reproduced by several, qualitatively different sets of parameters, this procedure may easily lead to misinterpretations.

Therefore, it is important to realize the origin and reliability of the various parameters, as well as their relevance within the present context.

The desorption (kink) energies for the mono-, bi-, and multilayer were determined from a leading edge analysis of the thermal desorption spectra, just like the preexponential factor for motion perpendicular to the surface (i.e., the attempt frequency for desorption). Thus, these parameters are comparably accurate and reliable, whereas lateral interactions, transition-state energies, and attempt frequencies for diffusion parallel to the surface cannot be obtained from a simple leading-edge analysis of the desorption spectra.

Desorption of Xe/Pt(111) has been shown to take place in 2D quasiequilibrium.[43] This should also be true for Xe adsorbed on the much smaller (111) terraces of the Pt(997) surface. Equilibrium is ensured if the particles can overcome all transition states within a reasonable time, i.e., if all diffusion processes are highly active. In this case, neither the diffusion attempt frequencies nor the exact values of the transition-state energies will influence the behavior of the system. Thus, the transition states for desorption simulations have been chosen as high as possible (to increase the calculation speed by avoiding needless jumps), but as low as necessary to guarantee that the system is able to maintain 2D equilibrium.

For studying adsorption, simple and reasonable transition-state energies and attempt frequencies have been chosen. Since the real, unknown values might be different and much more complex (e.g., depend on site, neighborhood, temperature, etc.), one cannot expect the simulation to provide unambiguous results for adsorption experiments at very low temperatures.

Finally, the measured kink energies have to be divided into adsorbate-substrate and lateral adsorbate-adsorbate contributions, respectively. At least a clear distinction between attractive and repulsive lateral interactions can be made on the basis of the shape (order) of the desorption curves.[42] In the case of Xe/Pt(997), the high-temperature shoulder in Fig. 8 exhibits a second-order-like behavior. This indicates a relatively strong lateral *repulsion* within the energetically most preferable row. On the other hand, the zero-order desorption behavior of the main peak of Xe/Pt(111) can be taken as evidence for *attractive* lateral interactions on the terraces.

In the present case, the information on the parameter values is incomplete. Therefore, we do not attempt to determine all remaining unknowns; nor do we pretend that such an unambiguous determination would be possible. Instead, we focus on the four parameter sets in Table I, which are based on earlier proposals. We find that among the four models only model No. 4 can quantitatively reproduce the experimentally observed adsorption *and* desorption behavior for Xe/Pt(997). The impact of the simulation results on our understanding of the Xe/Pt(997) system with respect to interaction strengths, adlayer structure, and preferential growth is discussed below.

B. Comparison with the experimental data

Comparing the results of the KMC simulation with the available experimental adsorption[6,7] and desorption[5] data we can draw the following conclusions:

(i) The desorption of Xe from the Pt(111) surface is well reproduced assuming a binding energy of about 256 meV and a lateral interaction of $3E_{lat}=21$ meV. This corresponds to a total binding energy of 271 meV in the 2D-gas–solid coexistence regime. Both values compare quite well with the measured isosteric heats of adsorption of $Q_0=260\pm15$ meV at low coverage and $Q_1=298\pm22$ meV for the unconstrained monolayer. However, the effective nearest-neighbor interaction between two Xe atoms of only 7 meV is surprisingly small as compared to the values of 11–15 meV expected from the experiment. As discussed in Sec. III this large difference could be due to the incomplete modeling of the Xe-Xe interaction. Both the long-range nature and the elastic strain of small 2D Xe islands are expected to increase the density of the 2D Xe gas which is required to correctly reproduce the initial first-order desorption behavior. On the basis of the KMC simulations we can rule out kinetic effects to be responsible for the first-order desorption at low coverages, since it would demand an unphysically large barrier for diffusion of a single Xe adatom.

(ii) The KMC simulations on the adsorption and desorption of Xe on the vicinal Pt(997) surface provide interesting information on the binding at the Pt step edges. Obviously these step edges present *two* energetically favored sites promoting the sequential growth of two Xe rows. This situation is well described by model No. 4 where the preferred adsorption sites are located on top (398 meV) and at the bottom (287 meV) of the Pt step edges. These values are deduced from the analysis of the peak position of the high-temperature feature in the desorption spectra. Furthermore, the peak width and the pronounced shift towards lower temperature with increasing coverage (step decoration) reveals a sizable repulsive interaction between Xe atoms adsorbed within the energetically most favored edge row. A value of -15.9 meV together with the other parameters listed in Table I gives a quantitative fit of the edge desorption feature.

In addition to the system energetics and step interaction, our analysis also provides indirect information on the Xe adlayer structure on Pt(997).

First, we may conclude that the Xe adlayer on Pt(997) forms an aligned phase, with five close-packed rows per terrace at monolayer completion, rather than a $(\sqrt{3}\times\sqrt{3})R30°$ phase as on extended Pt(111) terraces. This can be inferred from the relative area of the step-desorption and terrace-desorption peaks but also from the observed row-by-row growth as explained in Sec. IV. In fact, it is quite intuitive that the strong binding to the step edge will favor a densely packed (aligned) Xe row instead of one with a Xe spacing of $3a_{Pt}$. This provides the driving force for the formation of an aligned phase on the small terraces of the Pt(997) surface.

In addition, we find evidence for the preferential adsorption and successive decoration of two rows at the Pt step edges. An energetic argument that another (second) row should be energetically favored was already put forward in Ref. 6. There it was assumed that both rows were located at the lower step edge rather than at either side of the step. In fact, both situations should give rise to the same adsorption and desorption scenario.[54] Yet the additional binding strength

of a Xe atom in the second row as compared to the terrace sites must be sufficiently strong in order to give rise to a distinct second-row growth at finite temperature. In fact, this excess energy has been estimated to be about 18 meV,[6] which is significantly larger than the 5 meV calculated in Ref. 7 (see model No. 2) for the van der Waals attraction of the step edge at the position of the second Xe row on the terrace. Evidently, this is not an issue if one assumes that both the first and second rows in question are located in the intermediate neighborhood of the step edge—one on top and the other at the bottom. In fact, the associated excess binding energy in the bottom row (23 meV in model No. 4) is in good agreement with the experimental estimate.

The fact that the first Xe row on Pt(997) grows with a spacing of $2a_{Pt}=5.54$ Å rather than at the nearest-neighbor distance of 4.3 Å or smaller (in order to benefit from the strong attraction to the step edge) clearly indicates a lateral repulsion between the Xe atoms within this row. This situation is, indeed, reminiscent of the Xe/Pt(111) system where such a repulsion was observed in for the adsorption of Xe on top of the residual step edges.[17,18] Certainly, the binding situation at the step edges on the vicinal Pt(997) could be different than on Pt(111). Yet the step interaction parameters in Table I derived for the Pt(997) surface give an equally good account for the influence of the residual step edges on the Pt(111) surface, where the step density is only 0.5%. This suggests that the binding situation at the step edges on the vicinal Pt(997) is rather similar to the case of Pt(111) where the steps are much further apart.

Finally, the presence of distance-2 commensurate edge structure raises another question on the growth scenario of Xe on the Pt(997) surface. Just as for the $(\sqrt{3}\times\sqrt{3})R30°$ structure in model Nos. 1 and 2 an expanded interatomic distance within the first Xe row would introduce a lattice mismatch with respect to a second (closed-packed) row growing in direct contact with the first one. As shown in Sec. IV the lateral interactions favoring a spacing of 4.3 Å rather than 5.54 Å would impede the formation of a complete second row and lead to an incomplete wetting, i.e., 2D island formation on the terraces. This problem does not arise if the two rows are located on the top and at the bottom of the step edge with only a weak interaction between the two rows (actually zero in model No. 4).

Another issue concerning the growth scenario is to what extent the sequential adsorption or row-by-row growth is governed by equilibrium thermodynamics or surface kinetics. Comparing the growth at different temperatures (especially for model No. 4; see Fig. 7), we find that a perfect row-by-row growth is only achieved at rather high temperatures, whereas the experiment reveals a distinct second-row growth down to about 40 K.[6] In fact, at lower temperatures ($\leqslant 60$ K) the simulation predicts an almost simulataneous formation of the first and second rows. This is due to the limited mobility of the Xe atoms, which have to surmount a barrier of $368-287=81$ meV to escape from the bottom row in order to reach the energetically favored top row. In other words, Xe atoms impinging on the terrace will reach the nearest bottom or top row at either side of the terrace with equal statistical probability and become confined within these two rows. Lowering the Ehrlich-Schwoebel barrier (between the top and bottom rows) would result in the thermodynamically favored row-by-row growth at lower temperature and remedy the remaining discrepancy with the experiment.

In addition, we should emphasize that the mobility of the rare gases often appears to be larger than expected on the basis of realistic estimates for the diffusion barrier.[12,19] This phenomenon has been attributed to a so-called transient or hyperthermal mobility: Xe atoms trapped on the metal surface cannot readily accommodate the adsorption energy which is thus transformed into a substantial kinetic energy. This allows a trapped Xe atom to move large distances even at cryogenic temperatures until it eventually thermalizes, e.g., at step edges,[12] impurities, or Xe islands that have already formed on the surface.[13] This excess energy could actually allow Xe atoms arriving at the bottom row to reach an unoccupied neighboring site within the top row. Indeed, STM images recorded after Xe deposition on a Pt(111) surface show an almost exclusive decoration of the top of the step edges at 13 K before island nucleation at the bottom edge[17,18] sets in. Likewise, large monolayer deep vacancy islands prepared by ion sputtering and subsequent annealing remain completely unfilled up to relatively high coverage. These observations suggest that Xe atoms impinging on a terrace can reach a neighboring step where they are lifted up onto the upper step edge.

VII. CONCLUSION

Kinetic Monte Carlo simulations offer a powerful tool to study and analyze growth and desorption phenomena of adsorbed particles on crystal surfaces. They allow one to establish a direct connection between the interaction potentials and the behavior of a large ensemble of particles and, hence, to connect between theory and experiment.

The unusual desorption behavior of Xe on Pt(111) was interpreted in terms of a surprisingly low lateral Xe-Xe interaction of 7 meV, rather than by kinetic constraints or a reduced adsorbate mobility. The small ''effective'' lateral interaction could be an artifact arising from the nearest-neighbor model which neglects the long-range nature of the Xe-Xe interaction and surface-mediated or three-body interactions, as well as the possible influence of the lattice strain.

The adsorption of Xe/Pt(997) has been studied using four different structure and interaction models based on previous suggestions in the literature. As a result, we can rule out the formation of a $(\sqrt{3}\times\sqrt{3})R30°$ adlayer structure on the terrace in favor of an aligned incommensurate phase as suggested by LEED and He diffraction. Furthermore, we conclude that two Xe rows are energetically favored with respect to the terrace sites. We can find a set of parameters (model No. 4 in Table II), which is able to reproduce the experimentally observed sequential growth of the first two Xe rows per Pt terrace. In this model the row on top and (to a lesser extent) the row at the bottom of each Pt step edge are energetically preferred and the Xe atoms adsorbed within the top row experience a local lateral repulsion.

The *same* set of parameters has been successfully used to describe the desorption of Xe/Pt(997) as well as the influence of the residual step edges on the Pt(111) surface. The simulated TPD spectra match *quantitatively* to the experimental ones.

ACKNOWLEDGMENTS

This project was supported by the Austrian Fonds zur Förderung der wissenschaflichen Forschung under Contract Nos. P12317-NAW and P14628-TPH.

*Electronic address: zeppenfeld@exphys.uni-linz.ac.at

[1] P. Zeppenfeld, in *Noble Gases on Metals and Semiconductors*, edited by H.P. Bonzel, Landolt Börnstein, New Series, Group III, Vol. 42, Pt. A1 (Springer, Berlin, 2001), p. 67.
[2] G. Vidali, G. Ihm, H.-Y. Kim, and M.W. Cole, Surf. Sci. Rep. **12**, 133 (1991).
[3] L.W. Bruch, M.W. Cole, and E. Zaremba, *Physical Adsorption: Forces and Phenomena* (Clarendon Press, Oxford, 1997).
[4] C.T. Rettner, D.S. Bethune, and E.K. Schweizer, J. Chem. Phys. **92**, 1442 (1990).
[5] W. Widdra, P. Trischberger, W. Frieß, D. Menzel, S.H. Payne, and H.J. Kreuzer, Phys. Rev. B **57**, 4111 (1998).
[6] V. Marsico, M. Blanc, K. Kuhnke, and K. Kern, Phys. Rev. Lett. **78**, 94 (1997).
[7] V. Pouthier, C. Ramseyer, C. Girardet, K. Kuhnke, V. Marsico, M. Blanc, R. Schuster, and K. Kern, Phys. Rev. B **56**, 4211 (1997).
[8] F. Picaud, V. Pouthier, C. Ramseyer, and C. Girardet, Surf. Rev. Lett. **6**, 669 (1999).
[9] K. Wandelt, J. Hulse, and J. Küppers, Surf. Sci. **104**, 212 (1981).
[10] R. Miranda, S. Daiser, K. Wandelt, and G. Ertl, Surf. Sci. **131**, 61 (1983).
[11] H.R. Siddiqui, P.J. Chen, X. Guo, and J.T. Yates, Jr., J. Chem. Phys. **92**, 7690 (1990).
[12] P.S. Weiss and D.M. Eigler, Phys. Rev. Lett. **69**, 2240 (1992).
[13] P. Zeppenfeld, J. Goerge, M. Büchel, R. David, and G. Comsa, Surf. Sci. **318**, L1187 (1994).
[14] J.C. Tully, Surf. Sci. **111**, 461 (1981); Faraday Discuss. Chem. Soc. **80**, 300 (1995).
[15] M. Head-Gordon and J.C. Tully, Surf. Sci. **268**, 113 (1992).
[16] H. Schlichting, D. Menzel, T. Brunner, and W. Brenig, J. Chem. Phys. **97**, 4453 (1992).
[17] P. Zeppenfeld, S. Horch, and G. Comsa, Phys. Rev. Lett. **73**, 1259 (1994).
[18] S. Horch, P. Zeppenfeld, and G. Comsa, Appl. Phys. A: Mater. Sci. Process. **60**, 147 (1995).
[19] M. Dienwiebel, P. Zeppenfeld, J. Einfeld, G. Comsa, F. Picaud, Ch. Ramseyer, and C. Girardet, Surf. Sci. **446**, L113 (2000).
[20] Ch. Arumainayagam *et al.*, Surf. Sci. **226**, 180 (1990); J. Chem. Phys. **95**, 5437 (1991).
[21] C.T. Rettner, C.B. Mullins, D.S. Bethune, D.J. Auerbach, E.K. Schweizer, and W.H. Weinberg, J. Vac. Sci. Technol. A **8**, 2699 (1990).
[22] D.L. Meixner and S. George, J. Chem. Phys. **98**, 9115 (1993).
[23] B. Poelsema, L.K. Verheij, and G. Comsa, Surf. Sci. **152/153**, 851 (1985).
[24] K. Kern, R. David, R.L. Palmer, and G. Comsa, Surf. Sci. **175**, L669 (1986).
[25] K. Kern, R. David, P. Zeppenfeld, and G. Comsa, Surf. Sci. **195**, 353 (1988).
[26] K. Kern and G. Comsa, in *Phase Transitions in Surface Films 2*, Vol. 267 of *NATO Advanced Study Institute, Series B: Physics*, edited by H. Taub *et al.* (Plenum Press, New York, 1991), p.41.
[27] K. Kern, Phys. Rev. B **35**, 8265 (1987).
[28] K. Kern, R. David, P. Zeppenfeld, R.L. Palmer, and G. Comsa, Solid State Commun. **62**, 391 (1987).
[29] A. Cassuto, J.J. Ehrhardt, J. Cousty, and R. Riwan, Surf. Sci. **194**, 579 (1988).
[30] M. Potthoff, G. Hilgers, N. Müller, U. Heinzmann, L. Haunert, J. Braun, and G. Borstel, Surf. Sci. **322**, 193 (1995).
[31] Th. Seyller, M. Caragiu, R.D. Diehl, P. Kaukasoina, and M. Lindroos, Phys. Rev. B **60**, 11 084 (1999).
[32] S. Horch, P. Zeppenfeld, and G. Comsa, Surf. Sci. **331-333**, 908 (1995).
[33] J. Ellis, A.P. Graham, and J.P. Toennies, Phys. Rev. Lett. **82**, 5072 (1999).
[34] B. Hall, D.L. Mills, P. Zeppenfeld, K. Kern, U. Becher, and G. Comsa, Phys. Rev. B **40**, 6326 (1989).
[35] L.W. Bruch, A.P. Graham, and J.P. Toennies, J. Chem. Phys. **112**, 3314 (2000).
[36] J.E. Black and A. Janzen, Phys. Rev. B **39**, 6238 (1989); Surf. Sci. **217**, 199 (1989).
[37] P.A. Rejto and H.C. Andersen, J. Chem. Phys. **98**, 7636 (1993).
[38] D.S. Bethune, J.A. Barker, and C.T. Rettner, J. Chem. Phys. **92**, 6847 (1990).
[39] J.A. Barker, C.T. Rettner, and D.S. Bethune, Chem. Phys. Lett. **188**, 471 (1992).
[40] J. Barker and C.T. Rettner, J. Chem. Phys. **97**, 5844 (1992); **101**, 9202 (1994).
[41] J.E. Müller, Phys. Rev. Lett. **65**, 3021 (1990).
[42] B. Lehner, M. Hohage, and P. Zeppenfeld, Surf. Sci. **454-456**, 251 (2000).
[43] B. Lehner, M. Hohage, and P. Zeppenfeld, Chem. Phys. Lett. **336**, 123 (2001).
[44] J.F. Fernández and J. Rivero, Comput. Phys. **10**(1), 83 (1996).
[45] K.A. Fichthorn and W.H. Weinberg, J. Chem. Phys. **95**, 1090 (1991).
[46] The phase diagram of Xe/Pt(111) has been studied in great detail (see, e.g., Refs. 26–28). The $(\sqrt{3}\times\sqrt{3})R30°$ commensurate phase is stable at temperatures $T>62$ K and coverages $\Theta \leqslant 1/3$. At lower temperature and higher coverage, incommensurate domain-wall phases with either striped or hexagonal symmetry are observed.
[47] Simulations with different diffusion saddle points have been performed for this system. The effect of a 150 meV diffusion barrier, for instance, is barely visible in the monolayer desorption spectra.
[48] T.L. Hill, *Statistical Mechanics* (McGraw-Hill, New York, 1956).
[49] M.B. Webb and L.W. Bruch, in *Interfacial Aspects of Phase Transformations*, edited by B. Mutaftschiev, Vol. 87 of *NATO Advanced Study Insititute, Series C* (Reidel, Dordrecht, 1982), p. 365.
[50] B. Lehner, M. Hohage, and P. Zeppenfeld (unpublished).

[51] K.A. Fichthorn and M. Scheffler, Phys. Rev. Lett. **84**, 5371 (2000).
[52] K. Kern, R. David, R.L. Palmer, and G. Comsa, Phys. Rev. Lett. **56**, 620 (1986).
[53] P. Trischberger, H. Dröge, S. Gokhale, J. Henk, H.-P. Steinrück, W. Widdra, and D. Menzel, Surf. Sci. **377-379**, 155 (1997).
[54] The major argument in Ref. 7 to propose the bottom of the step edge to be occupied first was the overall intensity of the specular He intensity and the shift of the diffraction satellites towards larger exit angles after completion of the first Xe row. In our understanding, both observations are quite compatible with adsorption on top of the step edges. First, the pronounced intensity drop of the specular peak during formation of the first row indicates an exposed adsorption site on the upper terrace rather than within the ''shadow'' at the bottom of the diffusely scattering step edge. Second, one would expect a bending towards larger exit angles of the trajectories of those He atoms which after being diffracted from the flat part of the terraces experience the attractive potential of a Xe atom located on top of the step edge during their way out.